

Radio-wave propagation in the non-Gaussian interstellar medium

Stanislav Boldyrev¹ and Carl R. Gwinn²

¹*Department of Astronomy and Astrophysics, University of Chicago,
5640 S. Ellis Ave, Chicago, IL 60637; boldyrev@uchicago.edu*

²*Physics Department, University of California at Santa Barbara, CA 93106;
cgwinn@physics.ucsb.edu*

ABSTRACT

Radio waves propagating from distant pulsars in the interstellar medium (ISM), are refracted by electron density inhomogeneities, so that the intensity of observed pulses fluctuates with time. The observed pulse shapes are used to diagnose electron-density distribution in the ISM. The theory relating the observed pulse time-shapes to the electron-density correlation function has developed for 30 years, however, two puzzles have remained. First, observational scaling of pulse broadening with the pulsar distance is anomalously strong; it is consistent with the standard model only when non-uniform statistics of electron fluctuations along the line of sight are assumed. Second, the observed pulse shapes are consistent with the standard model only when the scattering material is concentrated in a narrow slab between the pulsar and the Earth.

We propose that both paradoxes are resolved at once if one assumes stationary and uniform, but *non-Gaussian* statistics of the electron-density distribution in the interstellar medium. Such statistics must be of Lévy type, and the propagating ray should exhibit a Lévy flight rather than the Gaussian random walk implied by the standard model. We propose that a natural realization of such statistics may be provided by the interstellar medium with random electron-density discontinuities. A Lévy distribution has a divergent second moment, therefore, the standard approach based on the electron-density correlation function does not apply. We develop a theory of wave propagation in such a non-Gaussian random medium, and demonstrate its good agreement with observations. The qualitative introduction of the approach and the resolution of the anomalous-scaling paradox was presented earlier in [PRL **91**, 131101 (2003); ApJ **584**, 791 (2003)].

Subject headings: ISM: general—pulsars: general—scattering—MHD—turbulence

1. Introduction.

Observations of pulsar signals provide a valuable tool for investigating electron density distribution in the interstellar medium. The pulsar intrinsic signal is narrow in time, being about few percent of the pulsar period. The observed signal (averaged over many periods of pulsation) is broad and asymmetric with a sharp rise and a slow decay. The pulse broadening is attributed to the random refraction the waves experience while propagating in the interstellar medium.

1.1. Overview.

The shapes of the signals, and their scalings with wavelength λ and with the pulsar distance have been investigated observationally and analytically for 30 years. The standard theory of interstellar scintillations (described in detail below) assumes that the propagating wave is refracted by random Gaussian gradients, thought to be a good approximation due to the central limit theorem (Tatarskii 1961). The symmetric Gaussian distribution is fully characterized by its second moment, and the standard theory of scintillations aimed at reconstructing this moment from observations. The contradictions of this theory with observations were noted in the early 1970's, although not many pulsars were investigated at that time to make a definitive conclusion.

The signal shape is characterized by its time-width, τ , estimated at the $1/e$ level. In 1971, Sutton analyzed scalings of pulse broadening times, τ , with the radio wavelength, λ , and with dispersion measures, DM , corresponding to the pulsar's distance along the line of sight, $DM = \int dz n(z)$. Observational scaling for large dispersion measures, $DM > 30 \text{ pc cm}^{-3}$, is close to $\tau \propto \lambda^4 DM^4$, while the theory gave $\tau \propto \lambda^4 DM^2$. The recent observational results are shown in Fig. (1). To overcome the difficulty with the anomalous DM-scaling, Sutton suggested that the interstellar turbulence was not statistically uniform along the lines of sight, so that the lines of sight for more distant pulsars intersected regions with stronger turbulence.

The second paradox was encountered by Williamson (1972, 1973, 1974), who compared the observed shapes of the pulses with the shapes predicted by the standard theory. He obtained a surprising result that the model of continuous turbulent medium was not consistent with observations. Rather, the best agreement was given by the models where all the scattering material was concentrated either in a thin screen or in a slab covering only 1/4 of the line of sight between the pulsar and the Earth, with nearly equal quality of fit to the data [see the discussion and Fig. 4 in (Williamson 1974)].

These two assumptions that are necessary to reconcile the standard theory with the observations may have physical grounds since the interstellar medium is not uniform and denser regions (with stronger turbulence) are encountered closer to the galactic center. However, in this paper we discuss a simple and perhaps more plausible physical explanation for the Sutton and Williamson paradoxes. According to this explanation, the Sutton and Williamson paradoxes are not the consequence of the non-uniform, large-scale galactic distribution of the electron density responsible for scattering. Rather, they reflect the universal properties of the microscopic structures of the density fluctuations.

1.2. Lévy flights. Mathematical background.

In our recent work (Boldyrev & Gwinn 2003a,b, 2004) we proposed that the Sutton paradox is the evidence of statistically uniform but *non-Gaussian* electron distribution in the interstellar medium. We noted that the time-broadened pulses belong to those observational objects that depend not on the moments of the electron-density distribution function, but on its full shape. The standard Gaussian approach did not recognize this fact because in the Gaussian case, knowledge of the second moment is equivalent to knowing the distribution function itself. However, for a general non-Gaussian electron-density distribution the second moment may formally diverge, and the electron-density correlation function may not characterize the pulse shape.

Physically, this divergence means that the second moment of ray-angle deviation is dominated not by the bulk of its distribution function, but by the extremely far cut-offs at the tails of this function [as we will see in the example of Section 4]. In contrast, the observed signal shape is determined by the bulk of the distribution function and is not sensitive to its far-tail cut-offs. In other words, the electron-density correlation function and the shape of the observed pulsar signal provide different, complementary descriptions of the electron distribution in the ISM.

We also note that in the Lévy model, the pulse shapes may provide a unique opportunity to diagnose plasma fluctuations at very small scales, $> 10^8$ cm. These scales can be smaller than the Coulomb mean-free path in HII regions, and can be close to the ion gyro radius. Observations of pulse shapes may thus provide diagnostics for magnetized plasma fluctuations, which may help to elucidate the role of magnetic fields in interstellar turbulence, see also (Armstrong, Rickett, & Spangler 1995; Goldreich & Sridhar 1997).

In the theory of scintillation, the quantity of interest is the transverse electron-density difference, averaged along the line of sight, $\Delta n_{\perp} = \int dz [n(\mathbf{x}_1, z) - n(\mathbf{x}_2, z)]$. A wave

propagating in the interstellar medium is scattered (refracted) by density inhomogeneities, and the statistics of the refraction angle is related to the statistics of density differences across the line of sight.

In the approach proposed in (Boldyrev & Gwinn 2003a,b) we assumed that the distribution function of Δn_{\perp} was stationary and uniform, but non-Gaussian, and it had a power-law decay as $|\Delta n_{\perp}| \rightarrow \infty$. If this distribution does not have a second moment, then the sum of many density differences along the line of sight does not have the Gaussian distribution, i.e. the Central Limit Theorem does not hold. Instead, the limiting distribution, if it exists, must be the so-called Lévy distribution, which is common in various random systems (Klafter, Zumofen & Shlesinger 1995). By construction, such a distribution is stable under convolution, i.e. the appropriately rescaled sum of two independent variables drawn from the same Lévy distribution, has again the Lévy distribution. The Gaussian distribution is a particular case of this more general stable distribution.

The Fourier transform (the characteristic function) of an isotropic Lévy probability density function, $P_{\beta}(\boldsymbol{\sigma})$, has the simple form,

$$F(\boldsymbol{\mu}) = \int_{-\infty}^{\infty} d\boldsymbol{\sigma} P_{\beta}(\boldsymbol{\sigma}) \exp(i\boldsymbol{\mu} \cdot \boldsymbol{\sigma}) = \exp(-|\boldsymbol{\mu}|^{\beta}), \quad (1)$$

where the Lévy index β is a free parameter, $0 < \beta \leq 2$. This form is valid for an arbitrary dimensionality of the fluctuating vector $\boldsymbol{\sigma}$. As we explain below, in our case this vector is two-dimensional, $\boldsymbol{\sigma} \propto \hat{\mathbf{y}} \int dz [n(z, \mathbf{x}_1) - n(z, \mathbf{x}_2)]$, where \mathbf{x} is the coordinate in the plane perpendicular to the line of sight, z , and $\hat{\mathbf{y}}$ is the unit vector in the direction connecting the two points in this plane, $\hat{\mathbf{y}} = \mathbf{y}/|\mathbf{y}|$, where $\mathbf{y} = \mathbf{x}_1 - \mathbf{x}_2$.

Equation (1) can be taken as the definition of the *isotropic* Lévy distribution, and in the present paper we will consider only isotropic distributions. However, it is important to note that a stable distribution need not be isotropic [see, e.g., (Nolan 2002)]. In the simplest case, the anisotropic distribution is a copy of the isotropic distribution, rescaled along one axis; but far less symmetric Lévy distributions are possible. Non-isotropic stable distributions might arise in the case of the magnetized interstellar medium, when wave scattering has one or several preferred directions. For example, anisotropic scattering may be characteristic of interstellar MHD turbulence, as described by Goldreich & Sridhar (1997); Lithwick & Goldreich (2001); Cho, Lazarian, & Vishniac (2000); Chandran & Backer (2002); Scalo & Elmegreen (2004), where the preferred direction is given by the large-scale magnetic field.

The sum of N Lévy distributed variables scales as $|\sum^N \boldsymbol{\sigma}| \sim N^{1/\beta}$, which becomes diffusion in the Gaussian limit $\beta = 2$. For $\beta < 2$, the probability distribution function has algebraic tails, $P_{\beta}(\boldsymbol{\sigma})\sigma d\sigma \sim |\boldsymbol{\sigma}|^{-1-\beta} d\sigma$, for large $|\boldsymbol{\sigma}|$, and its moments, $\langle |\boldsymbol{\sigma}|^{\zeta} \rangle$, of the order

$\zeta \geq \beta$ diverge. In (Boldyrev & Gwinn 2003a,b), we considered smooth density fluctuations, $\sigma \propto |\mathbf{x}_1 - \mathbf{x}_2|$, and the proposed Lévy statistics of ray-angle deviation lead to the pulse-broadening scaling $\tau \propto \lambda^4 DM^{(2+\beta)/\beta}$. This agrees with observations when $\beta \approx 2/3$, and provides a natural resolution to the Sutton paradox.

1.3. The results of the paper.

In this paper we consider scintillations produced by a general, non-smooth density fluctuations, $\sigma \propto |\mathbf{x}_1 - \mathbf{x}_2|^{\alpha/2}$; the limit of smooth density fluctuations corresponds to $\alpha = 2$. More precisely, exponent α denotes the scaling of the density-difference PDF defined in formula (1), i.e. this PDF should have the form $P_\beta(\sigma, y) \sim P_\beta(\sigma/y^{\alpha/2})/y^{\alpha/2}$. In the non-smooth case, the effective Lévy index that enters the expressions for angle deviations is different from β , and is given by $\gamma = \alpha\beta/2$, as is explained in formulae (9) and (17) below.

As we noted above, in the Lévy case the electron-density correlation function (or second order structure function) is contributed to by the far-tail cut-off of the electron-difference distribution function. We will denote the correlation-function scaling as $\langle \sigma^2 \rangle \propto |\mathbf{y}|^\delta$, where the scaling exponent, δ , is in general different and independent of the Lévy distribution scaling exponents α and β . The exponent δ is related to the Fourier spectrum of electron density fluctuations, $\langle |n(k)|^2 \rangle k^2 \propto k^{-\delta}$.

In the present paper we demonstrate that the proposed Lévy statistics of ray-angle deviations provide a resolution for the Williamson paradox as well. For this purpose we, first, develop a theory of wave propagation in a Lévy random medium by approximating the medium by a uniform series of scattering screens. Then, we provide a general method for constructing the pulse-broadening function for an arbitrary Lévy index γ . And finally, we compare our results with the observational signals of large-dispersion-measure pulsars, recently published by Bhat *et al* (2004) and by Ramachandran, *et al* (1997). We obtain that the observational shapes agree well with the predictions of our theory for a uniform medium with the Lévy index $\gamma \sim 2/3$ to 1, while they are inconsistent with the Gaussian theory corresponding to the Lévy index $\gamma = 2$.

We also discuss the effect of “over-scattering” which is inherent for the Lévy scintillations, because the time-signals have long algebraic tails that do not decay to zero during pulse periods. This effect is crucial for comparing analytical and observational data, as we show in Section 5.

For illustrative purposes, we also present a particular model of the density distribution that produces the Lévy statistics of scintillations. The proposed density distribution is

strongly spatially intermittent, and it can be visualized as follows. Imagine that the electron density is concentrated in separated regions that have sharp irregular boundaries. We make the simplest assumption that these boundaries are random, similar to randomly folded two-dimensional sheets or shocks. If one further assumes that the line of sight intersects the boundary at a random angle whose distribution is uniform in all directions, such a picture corresponds to the particular case of a Lévy distribution of Δn , with $\alpha = 2$, $\beta = 1$, the so-called Cauchy distribution. This distribution is rather distinct from the Gaussian one, and is close to the distribution that has been predicted in our theory.

1.4. Related models.

The importance of randomly oriented discontinuous objects that can be encountered across the line of sight has been emphasized in earlier theoretical work on scintillation, see e.g., (Lambert & Rickett 2000) and (Cordes & Lazio 2001). As noted by Lambert & Rickett (2000), sharp density discontinuities may characterize stellar wind boundaries, supernova shock fronts, boundaries of HII regions at the Strömgren radius, etc. They may also arise from supersonic turbulent motion. Rickett, Lyne, & Gupta (1997) proposed that similar highly intermittent density structures may be responsible for observed low-frequency modulations (fringes) of dynamic pulsar spectra.

The approach of Lambert & Rickett (2000) utilized the non-Kolmogorov spectra of discontinuous density fluctuations. Cordes & Lazio (2001) considered wave scattering by confined or heavily modulated screens (such as disks, filaments, etc.), when the statistics of angular deviations were generally assumed Gaussian, with parameters varying along the screens. Both papers discussed important aspects of non-Kolmogorov and spatially intermittent electron-density distribution in the ISM, however, they implied the existence of the second moments of the scattering-angle distributions. Therefore, in the earlier considerations, the effects that we discuss in the present paper could not be discovered.

As we demonstrate in section 4, sharp density discontinuities can, in fact, produce a non-Gaussian distribution of the scattering angle, whose second moment diverges. In our approach we exploit such intermittent density statistics in their full generality. To elucidate the universal role of Lévy distribution, we keep our consideration as simple as possible, assuming statistically uniform and isotropic scattering screens (although generalizations for the non-isotropic and non-uniform cases are possible). The presence of strongly-scattering structures is naturally represented in our model by slowly decaying, power-law tails of the scattering-angle distributions. Our model has a simple physical interpretation and provides a practical way of calculating pulse shapes and pulse scalings. Most importantly, it naturally

resolves both the Sutton and the Williamson observational paradoxes, in a manner that is simpler and complementary to the standard Gaussian picture.

The Lévy-flight model may also be relevant to observations of extreme scattering events, such as those reported by Fiedler *et al* (1987); Wolszczan & Cordes (1987); Stinebring *et al* (2001). Such events have been investigated theoretically, as by Rickett, Lyne, & Gupta (1997); Romani, Blandford, & Cordes (1987). We note that these theoretical studies invoke uncommon incidents of scattering much larger than typical values to explain these events. In this sense, these events are consistent with the Lévy model we develop here, which includes rare, large events in a statistically-stationary way. However, we do not yet know whether these phenomena might fit into a single model for interstellar scattering along with the common phenomena we discuss in this work. The answer might possibly depend on the details of the picture for turbulence in which the Lévy model is realized. Accordingly, we do not discuss the extreme scattering events in the present work.

2. Directed-wave propagation in a random medium.

To address the puzzles mentioned above we need to review the standard theory of interstellar scintillations. First, we note that in the interstellar plasma with typical electron density $n \approx 0.03 \text{ cm}^{-3}$, the electron plasma frequency is $\omega_{pe} = (4\pi ne^2/m_e)^{1/2} \approx 10^4 \text{ s}^{-1}$. This frequency is much smaller than the typical observational frequency of $10^8 - 10^9 \text{ Hz}$, and, therefore, the propagating wave scatters only by a small angle on the scale of density inhomogeneities. The Fourier amplitude of electric field, $\mathbf{E}(\omega, \mathbf{r}) = \int \mathbf{E}(t, \mathbf{r}) \exp(-i\omega t) d\omega$, obeys the following equation:

$$\Delta \mathbf{E} + \frac{\omega^2}{c^2} \mathbf{E} - \frac{\omega_{pe}^2}{c^2} \mathbf{E} = 0, \quad (2)$$

see, e.g., (Tatarskii 1961; Lee & Jokipii 1975a). We are not interested in polarization effects that are small in the considered approximation by a factor $\Omega_e/\omega \sim 10^{-8}$, where $\Omega_e = eB/(mc)$ is the electron-cyclotron frequency, therefore, we consider the scalar wave amplitude, $E(\omega, \mathbf{r})$.

Equation (2) can be reduced further, using the so-called parabolic approximation (Tatarskii 1961). Assuming that the wave propagates in the line-of-sight direction, z , we can separate the quickly changing phase of the wave from the slowly changing wave amplitude, $E(\omega, \mathbf{r}) = \exp(iz\omega/c)\Phi_\omega(z, \mathbf{x})$, where \mathbf{x} is a coordinate perpendicular to z . The equation for the wave amplitude Φ_ω reads:

$$\left[2i\frac{\omega}{c} \frac{\partial}{\partial z} + \Delta_\perp - 4\pi r_0 n(z, \mathbf{x}) \right] \Phi_\omega(z, \mathbf{x}) = 0, \quad (3)$$

where Δ_{\perp} is a two-dimensional Laplacian in the \mathbf{x} plane, and $r_0 = e^2/(m_e c^2)$ is the classical radius of the electron.

Following the approach of Uscinski (1974); Williamson (1975); Lee & Jokipii (1975a,b,c) we introduce the two-point function $I(\mathbf{r}_1, \mathbf{r}_2, t) = \Phi(\mathbf{r}_1, t)\Phi^*(\mathbf{r}_2, t)$, whose Fourier transform with respect to time is $I_{\Omega}(\mathbf{r}_1, \mathbf{r}_2) = 1/\sqrt{2\pi} \int d\omega \Phi_{\omega+\Omega/2}(\mathbf{r}_1)\Phi_{\omega-\Omega/2}^*(\mathbf{r}_2)$. For coinciding coordinates, $\mathbf{r}_1 = \mathbf{r}_2$, this function is the intensity of the radiation whose variation with time we seek. To find this function we need first to solve the equation for $V_{\omega, \Omega} \equiv \Phi_{\omega+\Omega/2}(\mathbf{r}_1)\Phi_{\omega-\Omega/2}^*(\mathbf{r}_2)$, which can be derived from Eq. (3). Assuming that $\Omega \ll \omega$, we obtain the following equation,

$$i \frac{\partial V}{\partial z} = -\frac{1}{2k_1} \frac{\partial^2 V}{\partial \mathbf{x}_1^2} + \frac{1}{2k_2} \frac{\partial^2 V}{\partial \mathbf{x}_2^2} + \frac{2\pi r_0}{k} \Delta n V, \quad (4)$$

where we denote $k = \omega/c$, $\Delta n = n(z, \mathbf{x}_1) - n(z, \mathbf{x}_2)$, and $\Delta k \equiv k_1 - k_2 = \Omega/c$.

Equation (4) is hard to solve since $n(z, \mathbf{x})$ is an unknown random function. The standard theory uses the fact that it takes many refraction events to appreciably deviate the ray trajectory, as we discussed in the introduction. Therefore, due to the central limit theorem, the ray deviation angle exhibits a Gaussian random walk. One can therefore assume that the density fluctuations are Gaussian with the specified second-order correlator $\langle [n(z_1, \mathbf{x}_1) - n(z_2, \mathbf{x}_2)]^2 \rangle = 2\kappa(\mathbf{x}_1 - \mathbf{x}_2)\delta(z_1 - z_2)$, where short correlation length in z direction is the mathematical expression of the fact that the ray becomes appreciably deviated only when it travels the distance much larger than the density correlation length (Tatarskii 1961; Lee & Jokipii 1975a,b,c; Rickett 1977, 1990). The correlation function $\kappa(y)$ is the two-dimensional Fourier transform of the spectrum of the density fluctuations. More precisely, if the three-dimensional spectrum of the density fluctuations is $D(k) = \langle |n_k|^2 \rangle$, then $\kappa(y)$ is the Fourier transform of $D(\mathbf{k}_{\perp}, k_z = 0)$ with respect to \mathbf{k}_{\perp} . When the density has a power-law spectrum, $D(k)k^2 \propto k^{-\delta}$, with $1 < \delta < 2$, then $\kappa(y) \propto y^{\delta}$.

As we mentioned in the introduction, the statistically uniform Gaussian model fails to reproduce the observational scaling of the broadening time, $\tau \sim \lambda^4 DM^4$. Numerous attempts to reproduce this scaling by using different spectra of density fluctuations within this model have not been successful either. The purely shock-dominated density distribution has the spectrum $\langle |n_k|^2 \rangle k^2 \propto k^{-2}$, while the Kolmogorov turbulence has the spectrum $\langle |n_k|^2 \rangle k^2 \propto k^{-5/3}$; the difference in the spectral exponents is rather small to have a considerable consequence. For various important aspects of the standard Gaussian scintillation theory we refer the reader to (Goodman & Narayan 1985; Blandford & Narayan 1985; Gwinn *et al* 1998; Lambert & Rickett 2000; Lithwick & Goldreich 2001). In other contexts, the theory of wave propagation in Gaussian random media was developed in Saul, Kardar & Read (1992); Jayannavar & Kumar (1982).

In the next section we formulate the problem by assuming that the refraction occurs in a series of discrete structures, refracting ‘screens’, that are statistically identical, independent, and placed uniformly along the line of sight. This setting is physically appealing since, as we have mentioned in the introduction, the refraction in the interstellar medium is consistent with the presence of spatially intermittent scattering structures, see e.g., (Lambert & Rickett 2000; Cordes & Lazio 2001). Moreover, this is the simplest setting when the problem admits an exact analytic solution that allows us to treat both Gaussian and Lévy cases on the same footing.

3. Multi-screen model of scintillations.

Let us assume that wave scattering occurs in a series of thin flat screens uniformly placed along the line of sight. Also, for simplicity assume that the incident wave is planar, although an analogous consideration can be made for spherical geometry as well. Each screen gives a contribution to the signal phase; if we denote the wave function just before the screen by $V^{in}(\mathbf{x}_1, \mathbf{x}_2)$, then the wave function right after the screen will be given by $V^{out}(\mathbf{x}_1, \mathbf{x}_2) = S(\mathbf{x}_1, \mathbf{x}_2)V^{in}(\mathbf{x}_1, \mathbf{x}_2)$. The phase function, S , can be found from Eq. (4),

$$S(\mathbf{x}_1, \mathbf{x}_2) = \exp \left(\frac{-2i\pi r_0}{k} \int_0^l dz [n(z, \mathbf{x}_1) - n(z, \mathbf{x}_2)] \right), \quad (5)$$

where the integration is done over the thickness of the phase screen, l . Between the phase screens, the wave propagation is free. Effecting the change of variables, $\mathbf{y} = \mathbf{x}_1 - \mathbf{x}_2$, and $\mathbf{x} = \mathbf{x}_1 + \mathbf{x}_2$, we rewrite the Eq. (4) in this region,

$$i \frac{\partial V}{\partial z} = \frac{\Delta k}{k^2} \left(\frac{\partial^2 V}{\partial \mathbf{y}^2} + \frac{\partial^2 V}{\partial \mathbf{x}^2} \right) - \frac{1}{k} \frac{\partial^2 V}{\partial \mathbf{x} \partial \mathbf{y}}. \quad (6)$$

In what follows we will be interested in the wave function, V , averaged over different realizations of the electron density in the phase screens. Due to space homogeneity, the averaged transfer function, $\bar{S} \equiv \langle S(\mathbf{x}_1, \mathbf{x}_2) \rangle$, should depend only on the coordinate difference \mathbf{y} . Since refraction affects only the \mathbf{y} dependence of the wave function, we can assume that the averaged wave function is independent of \mathbf{x} , $\langle V(z, \mathbf{x}_1, \mathbf{x}_2) \rangle = U(z, \mathbf{y})$. Taking into account the \mathbf{x} dependence would lead to more cumbersome formulas, although it would not qualitatively change the results. We therefore model the free propagation between the screens by

$$i \frac{\partial U}{\partial z} = \frac{\Delta k}{k^2} \frac{\partial^2 U}{\partial \mathbf{y}^2}. \quad (7)$$

To describe the scattering we need to specify the averaged phase function, \bar{S} . In the Gaussian case, one can assume that the screen width, l , is of the order of the characteristic length of the density fluctuations, l_0 , and therefore¹,

$$\bar{S} = \exp[-\lambda^2 r_0^2 l_0 \kappa(y)], \quad (8)$$

where $\lambda = 2\pi/k$. Assuming that the main contribution to the scattering comes from the scales, y , much smaller than the density correlation length, we can expand $\kappa(y) \approx \kappa_0(y/l_0)^\alpha$, where $\kappa_0 \sim l_0(\Delta n_0)^2$, and Δn_0 is a typical amplitude (say, rms value) of density fluctuations. For example, if density fluctuations arise due to passive advection by the Kolmogorov turbulence, then $\alpha = 5/3$. The smooth density field corresponds to $\alpha = 2$.

The situation is completely different in the Lévy case, when the second-order moment of the density integral in (6) diverges. We however can assume that the density difference has some scaling form, $\Delta n_\perp = \int_0^{l_0} [n(\mathbf{x}_1, z) - n(\mathbf{x}_2, z)] dz \sim l_0 \Delta n_0 (y/l_0)^{\alpha/2}$, and use the Lévy formula (1) to write the most general expression for the averaged phase function \bar{S} ,

$$\bar{S} = \exp(-|\lambda r_0 l_0 \Delta n_0|^\beta |y/l_0|^{\alpha\beta/2}). \quad (9)$$

In the Gaussian limit, $\beta = 2$, this formula reduces to the previous result (8). Similar to the Gaussian case, the exponent $\alpha/2$ has the meaning of the density-difference scaling with the point separation, however, it characterizes not the second moment (that does not exist), but the density-difference distribution function itself.

More precisely, for a chosen point separation \mathbf{y} , the projected density difference in the screen function (5),

$$\Delta\Phi = \lambda r_0 \int_0^{l_0} dz [n(z, \mathbf{x}_1) - n(z, \mathbf{x}_2)] = \lambda r_0 \Delta n_\perp, \quad (10)$$

should be drawn from a distribution function that depends only on the combination $\Delta\Phi/y^{\alpha/2}$. We also note that contrary to the Gaussian case, the quantity Δn_0 entering equation (9), does not correspond to the rms value of density fluctuations, since $\langle \Delta n_\perp^2 \rangle$ does not exist in the Lévy case. Rather, it denotes the typical width of the density-difference PDF, say the density difference at which this PDF decays by the factor $1/e$ compared to its maximum value. On the contrary, the rms value of Δn_\perp would be given by far, non-Lévy tails of this PDF, and would be much larger than Δn_0 .

¹The assumption $l \sim l_0$ is not necessary. The only assumption required for our consideration is $l_0 \lesssim l$, and the final results can be generalized for this case. This generalization would however require further assumptions about the scattering structures, which at the present level of understanding can hardly be justified.

Physically, the Lévy screen function in the form (9) could correspond to the distribution of the phase integral, $\Delta\Phi$, when the integration path intersects a random density discontinuity, say a sharp boundary of an ionized region. Such a random boundary may naturally arise as a result of turbulent advection in an ionized region, and numerical simulations could test this intriguing possibility. Our suggestion is based on a result that a smooth, randomly oriented boundary reproduces the particular form of the Lévy screen function (9) corresponding to $\beta = 1$, $\alpha = 2$. We will derive this result in the next section. In general, particular values of α and β depend on the physical realization of scattering screens, which is not completely understood and cannot be specified in this work. For our present purposes, we simply assume the general form of the screen function (9) and provide a method for calculating the shape and the scaling of the received signal.

Let us consider a series of such screens placed along the line of sight, z , perpendicular to it, such that the distance between two adjacent screens is z_0 . Number the screens from the source to the observer, and consider the m th screen. Denote as $U_m^{in}(y_m)$ the wave function just before the wave passes the screen, and $U_m^{out} = \bar{S}U_m^{in}$ this function just after the screen. Between the screens $m-1$ and m , the propagation is free, therefore, we obtain from equations (4) and (7),

$$U_m^{in}(y_m) = \frac{ik^2}{2\Delta k\pi z_0} \int \exp\left(\frac{-ik^2(\mathbf{y}_m - \mathbf{y}_{m-1})^2}{2\Delta k z_0}\right) \bar{S}(y_{m-1}) U_{m-1}^{in}(y_{m-1}) d^2 y_{m-1}. \quad (11)$$

We can write the wave function after the wave has passed N screens, by iterating this formula N times, and by using the expression for the screen function, (9),

$$U_N^{in}(y_N) = [-i\pi A\Delta k]^{-N} \int \exp\left([iA\Delta k]^{-1} \sum_{m=1}^N (\Delta \mathbf{y}_m)^2 - B^{\alpha\beta/2} \sum_{m=1}^{N-1} |y_m|^{\alpha\beta/2}\right) \times U_0(y_0) d^2 y_{N-1}, \dots, d^2 y_1 d^2 y_0 \quad (12)$$

where we introduced the short-hand notation: $A = 2z_0/k^2$, $B = |\lambda r_0 l_0 \Delta n_0|^{2/\alpha}/l_0$, and $\Delta \mathbf{y}_m = \mathbf{y}_m - \mathbf{y}_{m-1}$.

To do the integrals, we need first to make a simple transformation of formula (12). We will substitute the following identity,

$$\exp[(\Delta \mathbf{y}_m)^2/(iA\Delta k)] = -i\pi A\Delta k \int \exp(i\boldsymbol{\xi}_m \cdot \Delta \mathbf{y}_m - iA\Delta k \xi_m^2) d^2 \boldsymbol{\xi}_m, \quad (13)$$

for each Δy_m , into formula (12). Our ultimate goal is to find the time dependence of the pulse intensity at the N th screen, i.e., $I(t) = \int U_N(y_N = 0, \Delta k) \exp(i\Delta k c t) d\Delta k c$. We therefore change the order of integration and do the Δk -integral first. As the result we get:

$$I(t) = \int \exp\left(-B^{\alpha\beta/2} \sum_{m=1}^{N-1} |y_m|^{\alpha\beta/2} - i \sum_{m=1}^N \boldsymbol{\xi}_m \cdot \Delta \mathbf{y}_m\right) U_0(y_0) \times$$

$$\delta \left(t - A \sum_{m=1}^N \xi_m^2 / c \right) d^2 \xi_N \dots d^2 \xi_1 d^2 y_{N-1} \dots d^2 y_0. \quad (14)$$

Introducing the non-dimensional variables $\tilde{y}_m = y_m B$ and $\tilde{\xi}_m = \xi_m / B$, we rewrite formula (14) as follows:

$$I(t) = \int \exp \left(- \sum_{m=1}^{N-1} |\tilde{y}_m|^{\alpha\beta/2} - i \sum_{m=1}^N \tilde{\xi}_m \cdot \Delta \tilde{\mathbf{y}}_m \right) U_0(\tilde{y}_0 / B) \times \\ \delta \left(t - \frac{AB^2}{c} \sum_{m=1}^N \tilde{\xi}_m^2 \right) d^2 \tilde{\xi}_N \dots d^2 \tilde{\xi}_1 d^2 \tilde{y}_{N-1} \dots d^2 \tilde{y}_0. \quad (15)$$

In the rest of this section we will use only the non-dimensional variables, and will omit the tilde signs.

Now we are ready to do the y -part of the integral. For this we make a simple rearrangement in the sum $\xi_1(y_1 - y_0) + \dots + \xi_N(y_N - y_{N-1}) \equiv -y_0 \xi_1 + y_N \xi_N + y_1(\xi_1 - \xi_2) + \dots + y_{N-1}(\xi_{N-1} - \xi_N)$. Recalling that y_N should be set to zero, we are left with $\sum_{m=1}^N \xi_m \cdot \Delta \mathbf{y}_m = -y_0 \xi_1 - \sum_{m=1}^{N-1} \mathbf{y}_m \cdot \Delta \xi_{m+1}$, where $\Delta \xi_m = \xi_m - \xi_{m-1}$. To complete the y -integration, we simply use the Lévy formula (1), and get:

$$I(t) = \int \delta \left(t - \frac{AB^2}{c} \sum_{m=2}^N \xi_m^2 \right) P_{\alpha\beta/2}(\Delta \xi_N) \dots P_{\alpha\beta/2}(\Delta \xi_2) \tilde{U}_0(\xi_1 B) d^2 \xi_N \dots d^2 \xi_1, \quad (16)$$

where $\tilde{U}_0(\xi)$ is the Fourier transform of $U_0(y)$, P is the Lévy distribution function introduced in (1). The last step is to note that $d^2 \xi_N \dots d^2 \xi_2 = d^2 \Delta \xi_N \dots d^2 \Delta \xi_2$, which allows us to give a simple interpretation to formula (16).

Before discussing this interpretation, we note the quantum mechanical analogy of our approach. If we could assume that $B^{\alpha\beta/2} \propto z_0$, and $z_0 \propto 1/N$ in the limit when the number of screens increases, $N \rightarrow \infty$, but the line-of-sight length is constant (which would be natural for the Gaussian case), the integral that we calculated in (12) would formally become the Feynman-Kac path integral for the solution of the Schrödinger equation with the potential $\propto i|\mathbf{y}|^{\alpha\beta/2}$. The transition from (12) to (16) given by formula (13) is the transition from the coordinate to the momentum representation of this integral.

Naturally, in the Gaussian case one can find the shape of $I(t)$ either by doing the multiple integral in (16) or by solving the corresponding Schrödinger equation. The first approach was essentially adapted in (Uscinski 1974; Williamson 1975), the second one in (Lee & Jokipii 1975b). In our Lévy model we cannot assume that $B^{\alpha\beta/2} \sim 1/N$, therefore, we have to work with the general expressions (12)-(14). Although the general integral (12) is quite complicated, the quantity of interest, $I(t)$, which is calculated with the aid of this

integral, has a quite simple meaning, and its probabilistic interpretation (16) can be easily understood.

The δ -function in formula (16) means that the signal intensity $I(t)$ is the probability density function of the time delay, $\tau = AB^2 \sum_{m=1}^N \xi_m^2 / c$. The variable ξ_m is proportional to the deviation angle of the ray path from the z -axis, $\xi_m \propto \theta_m$. [This is clear from (13) since $\xi_m \propto \Delta \mathbf{y}_m / z_0$, and this will also be the case in the geometric-optics analysis of Section 4.] This angle is the sum of elementary angle deviations caused by each phase screen, viz $\xi_m = \xi_1 + \sum_{i=2}^m \Delta \xi_i$. The propagation time between two neighboring screens exceeds the propagation time along the z -axis by the amount $\Delta \tau = (z_0/c)[1 - \cos \theta_m] \propto \xi_m^2$, and to get the total time delay, τ , we need to sum up these individual time delays.

Formula (16) teaches us that each angle increment, $\Delta \xi_s$, has a Lévy distribution with the index $\gamma = \alpha\beta/2$, which provides a practical way of constructing the pulse broadening function $I(t)$ without doing the multiple integrals in (16). This is a Monte-Carlo-type method for multiple integration. Indeed, to find the effect caused by the interstellar medium, we can neglect the intrinsic pulse shape, i.e., we can assume that the initial angle of the planar wave is zero, $\xi_1 = 0$. Then the function $I(t)$ is the probability density function of the variable

$$\tau = \frac{z_0 [r_0 l_0 \Delta n_0]^{4/\alpha}}{2 l_0^2 \pi^2 c} \lambda^{2+4/\alpha} \sum_{m=2}^N \left[\sum_{s=2}^m \Delta \xi_s \right]^2, \quad (17)$$

where all the variables $\Delta \xi_s$ are distributed independently and identically according to the Lévy law with the index $\gamma = \alpha\beta/2$. The same expression was obtained in our previous work for the case $\alpha = 2$, although without a detailed derivation (Boldyrev & Gwinn 2003a,b, 2004). We remind that the scaling exponent α corresponds to the spatial scaling of the density field, as is defined in Eq. (9). The Gaussian case corresponding to $\alpha = 2$, $\beta = 2$ was originally considered by Williamson (1972). The Gaussian case corresponding to the Kolmogorov density fluctuations, $\alpha = 5/3$, $\beta = 2$ was considered by Lee & Jokipii (1975c); however, the central part of the signal $I(t)$ predicted by their model did not differ much from the Williamson case.

We do not know the analytic expression for the probability density function of τ . However, it can be calculated numerically, by the method described in (Chambers, Mallows, & Stuck 1976; Nolan 2002). The generated pulse shapes for different numbers of screens, N , seem to be universal when appropriately rescaled. We will construct such shapes and will compare them with observations in Section 5.

The scaling of the time delay τ , i.e. the approximate scaling of its probability density function, can be found from the following consideration. Using the expression for the scaling of the sum of Lévy distributed variables, $|\sum^N \Delta \xi| \sim N^{1/\gamma}$ (recall that the Central Limit

Theorem does not hold), we derive $\tau \propto \lambda^{2+4/\alpha} N^{(2+\gamma)/\gamma}$, where the number of screens is proportional to the distance to the pulsar, $N \propto DM$. The observational scaling, $\tau \propto \lambda^4 DM^4$, is reproduced for $\alpha \approx 2$, and $\beta \approx 2/3$, which shows that ray-deviating density fluctuations do not have a Gaussian distribution but rather a Lévy distribution with the index $\beta \approx 2/3$. This is the important result of the Lévy model of scintillations, and it resolves the Sutton paradox.

In the Section 5, we will demonstrate that the Williamson paradox is resolved naturally in the Lévy picture of scintillations as well. But before that, in the next section we would like to present a physical model of scintillations that can be easily visualized and that demonstrates the essence of our approach.

4. Scintillations caused by random density discontinuities

The intensity function $I(t)$ can be calculated for the phase-screen function (9), once the parameters α and β have been specified from the physics of the problem. As an important example, let us consider a particular case of Lévy phase screens, which we shall call Cauchy screens, when the values of these parameters can be derived directly. Let us assume that the interstellar medium is filled with separated ionized regions such that all of them have the same electron-density contrast with the ambient medium, Δn_0 . We also assume that these regions are randomly shaped and have sharp boundaries.

A propagating ray is then refracted by these random boundaries due to the Snell's law, $\eta_1 \sin(\theta_1) = \eta_2 \sin(\theta_2)$, where θ is the angle between the ray and the normal to the boundary, and $\eta = (1 - \omega_{pe}^2/\omega^2)^{1/2} \approx 1 - \omega_{pe}^2/(2\omega^2) = 1 - (2\pi)^{-1}\lambda^2 r_0 n$ is the refraction index. As we explained in the introduction, the interstellar parameters ensure that $\omega_{pe}^2/\omega^2 \ll 1$, and each refraction event results in a very small angle deviation, $\delta\theta = \theta_1 - \theta_2$. Expanding $\sin(\theta_1) = \sin(\theta_2 + \delta\theta)$ through the first order in $\delta\theta$, we get from the Snell's law

$$\delta\theta = (2\pi)^{-1}\lambda^2 r_0 \Delta n_0 \tan(\theta), \quad (18)$$

where $\Delta n_0 = n_1 - n_2$. The distribution of $\tan(\theta)$ can be found assuming (somewhat artificially) that the boundary normal is uniformly distributed over all directions in a half-space, at the point where it intersects the line of sight. Denote $\boldsymbol{\sigma} = \tan(\theta)\mathbf{n}$, where \mathbf{n} is a unit vector indicating the direction of the refraction in the plane perpendicular to the ray propagation. Then the distribution of $\boldsymbol{\sigma}$ is given in the polar coordinates by:

$$P(\boldsymbol{\sigma}) d\sigma d\phi = \frac{1}{2\pi} \frac{\sigma}{(1 + \sigma^2)^{3/2}} d\sigma d\phi. \quad (19)$$

Quite remarkably, this distribution is the two-dimensional Lévy distribution with the index $\beta = 1$, also known as the Cauchy distribution. Its Fourier transform follows from formula (1), $F(\boldsymbol{\mu}) = \exp(-|\boldsymbol{\mu}|)$, we leave the derivation of this result to the reader as an instructive exercise.

To apply this result we need to calculate the screen function (5). It can be done if we note that for the plane-like density discontinuity, the screen phase (10) is easily calculated, $\Delta\Phi = \lambda r_0 \int dz [n(z, \mathbf{x}_1) - n(z, \mathbf{x}_2)] = \lambda r_0 \Delta n_0 (\boldsymbol{\sigma} \cdot \mathbf{y})$. Since $\boldsymbol{\sigma}$ has the Cauchy distribution (19), the averaged screen function can be found with the aid of formula (1),

$$\bar{S} = \exp(-\lambda r_0 \Delta n_0 |\mathbf{y}|), \quad (20)$$

and we recover formula (9) with $l = l_0$, and with $\alpha = 2$, $\beta = 1$; the parameters are close to those that we have proposed for the interstellar scintillation on the observational grounds, i.e., $\alpha \approx 2$, $\beta \approx 2/3$. We expect that the observational scaling $\beta \approx 2/3$ would correspond to more complicated, realistic structure of the boundaries, possibly, with the fractal dimension larger than 2. Interstellar turbulence can indeed corrugate two-dimensional structures to make them have higher-than-two fractal dimensions, as is seen in numerical results and in observations of molecular clouds (Boldyrev 2002; Boldyrev, Nordlund & Padoan 2002; Kristsuk & Norman 2004; Elmegreen & Falgarone 1996); see also (Meneveau & Sreenivasan 1990; Constantin, Procaccia, & Sreenivasan 1991; Kraichnan 1991). We expect this effect to have implications for interstellar scintillations, and we plan to consider it in the future work.

An attentive reader has probably noticed that Eq. (18) for the angle deviation cannot be valid for the arbitrarily large $\tan(\theta)$. Indeed, the refraction angle θ_2 cannot exceed the critical angle, given by $\sin(\theta_c) = \eta_1/\eta_2$, which is obtained when $\theta_1 = \pi/2$, where we assume $\eta_2 > \eta_1$. To obtain the general formula for the angle deviation we need to expand $\sin(\theta_1) = \sin(\theta_2 + \delta\theta)$ in the Snell's law up to the second order in $\delta\theta$, which gives

$$\delta\theta = \tan^{-1}(\theta) \left[\sqrt{1 + \pi^{-1} \lambda^2 r_0 \Delta n_0 \tan^2(\theta)} - 1 \right]. \quad (21)$$

The distribution of $\delta\theta$ thus has a cut-off at $\delta\theta_c = (\lambda^2 r_0 \Delta n_0 / \pi)^{1/2}$. For example, if the electron density fluctuations are $\Delta n_0 \sim 10^{-2} \text{ cm}^{-3}$, we have $(2\pi)^{-1} \lambda^2 r_0 \Delta n_0 \sim 10^{-12} \lll 1$, which implies that formula (18) holds in the broad range of scales. Indeed, the distribution of $\sigma = 2\pi\delta\theta/(\lambda^2 r_0 \Delta n_0)$ follows the Cauchy law (19), therefore the distribution function of $\delta\theta$ is strongly peaked at small $\delta\theta$. This function has a maximum at $\delta\theta \sim (2\pi)^{-1} \lambda^2 r_0 \Delta n_0 \sim 10^{-12}$, and a long asymptotic power-law tail, $P(\delta\theta) \propto 1/(\delta\theta)^2$, that spans about six orders of magnitude before it reaches the cut-off at $\delta\theta_c \sim 10^{-6}$.

This consideration provides an illustration to the main idea of our approach. The second moment of the distribution of $\delta\theta$ depends not on the shape of the distribution function (19),

but on the cut-off value of its asymptotic power-law tail, $\delta\theta_c$. On the contrary, the shape of the pulsar signal is determined by the full shape of the distribution function (19), and is practically independent of the large cut-off value $\delta\theta_c$.

5. Comparison with observations.

In Fig. (2) we present the pulse-broadening function, $I(t) = \langle \delta(t - \tau) \rangle$ which is the distribution function of the time delay, τ , given by formula (17), for the standard Gaussian model, $\alpha = 2, \beta = 2$, for the Lévy-Cauchy model, $\alpha = 2, \beta = 1$, and for the Lévy model with $\alpha = 2, \beta = 2/3$. Note that, in comparison with the pulse through a Gaussian medium, the Lévy models predict relatively greater intensity at short delays from the arrival time for the original pulse, as well as power-law tails at long delays. These tails result from rare, large occurrences of scattering.

We generated the two-dimensional isotropic Lévy distribution of $\Delta\xi_s$ using the methods of Feller (1971); Chambers, Mallows, & Stuck (1976); Nolan (2002). Let $\mathbf{X} = (X_1, X_2)$ be a Gaussian random vector, i.e. both components X_1 and X_2 are independent, identically distributed, one-dimensional Gaussian variables. Let Y be a completely skewed (i.e. positive), independent Lévy distributed variable corresponding to the Lévy index $\gamma/2$. This variable can be numerically generated using the method by Chambers, Mallows, & Stuck (1976), see also (Nolan 2002). Then the variable $\Delta\xi = \mathbf{X}\sqrt{Y}$ has an isotropic two-dimensional Lévy distribution with the index γ ; the proof can be found, e.g., in (Feller 1971). To generate an anisotropic Lévy distribution with uniform index γ (as may be relevant for the magnetized interstellar medium) one may choose an anisotropic Gaussian vector \mathbf{X} , and then proceed as above. In our present work we consider only isotropic distributions.

We compared the predicted pulse shapes with the data recently published in (Bhat *et al* 2004) and in (Ramachandran, *et al* 1997). Out of the 76 pulsars analyzed by Bhat *et al* (2004), we considered those with broad signals, in order to minimize the intrinsic-pulse effects. Good examples are provided by the four pulsars, P1849+0127 at 430 MHz (DM=214.4), J1852+0031 at 1175 MHz (DM=680.0), J1905+0709 at 430 MHz (DM=269.0), and P1916+0844 at 430 MHz (DM=339.0), where higher-frequency observations indicate that the intrinsic signal may be narrow. The dispersion measures are given in the units of $\text{pc} \cdot \text{cm}^{-3}$. Shapes of all of the pulses have a characteristic sharp rise and a narrow, pointed apex, which is inconsistent with the Gaussian model, in exact agreement with the observations by Williamson (1974) [see Fig. (4) in Williamson's paper]. On the contrary, our Lévy model provides a good fit to such shapes. For another similar comparison we used the pulse shape of J1848-0123 (DM=159.1) observed at 327 MHz by Ramachandran, *et al*

(1997); and we present this comparison in Figs. 4,5 as the illustrative example.

When making the comparisons, we tried to match the central parts of the observational and analytical curves. However, this was possible only when we shifted the zero level of the analytical curves down, as is shown by the thin solid lines in Fig. (4). This may be natural for “over-scattered” profiles, i.e., when the signal has a long tail that does not approach zero during the pulse period. This is exactly the case for our Lévy model. Besides, other observational effects, including noise from the sky and the telescope itself, usually prevent one from determining the baseline unambiguously.

We note that for a precise comparison, we must convolve the calculated pulse-broadening function with the narrow intrinsic shape of the pulse, and with the response function of the receiving system Ramachandran, *et al* (1997); Bhat, Cordes & Chatterjee (2003). This will lead to slight broadening of the predicted pulse profile, making the Gaussian model even less consistent with the observations.

The effects of over-scattering on baseline have not been considered observationally. This effect is important for comparison of our theory with observations, and we plan to investigate it in future work. Interferometry can distinguish between sky and telescope noise, and the overscattered tail of the pulse; comparison of the correlated flux density at the peak of the pulse, and between pulses, thus provides a measure of the parameter γ in Figures 2 and 3.

We are proceeding with additional observational tests that can distinguish among models for scattering. As Figures 2,3 suggest, different values of γ yield different delays between the arrival time for the unscattered pulse and the peak of the pulse, as well as different behavior in the tail. Observations at short wavelengths yield the arrival time for the unscattered pulse, with corrections for dispersion in the uniform interstellar plasma. Thus, multi-frequency observations of pulse broadening, with timing information, can distinguish among the different models.

Shapes of scattered images provide another possible observational test of our theory. As Equation (9) suggests, the distribution of deflections of waves, at a given point, is drawn from a Lévy distribution. Because the Lévy distribution is a stable attractor, iteration of the process yields a Lévy distribution of directions, at any distance from the source. Compared with a Gaussian distribution of similar width, a Lévy distribution has excesses at both large and small angles: it produces large deflections more commonly, and compensates with a large population with small deflection. Thus, the scattered image for a Lévy flight should have a halo at large angles, and a cusp at small angles, compared with a Gaussian image. Interestingly, observations of some heavily-scattered extragalactic sources show such core-halo excesses (Desai & Fey 2001). Intrinsic structure of the source could possibly explain

the observed halo structure; but cannot explain the relatively less-scattered cusp.

6. Discussions and conclusions.

In the present paper, we have investigated the observational pulse shape. Another object directly related to the electron distribution function is the visibility function, $\langle \Phi(\mathbf{x}_1, t)\Phi^*(\mathbf{x}_2, t) \rangle$, measured at the locations \mathbf{x}_1 and \mathbf{x}_2 at the Earth. However, the electron fluctuations probed by this function are limited to small scales, $|\mathbf{x}_1 - \mathbf{x}_2| \lesssim 10^8 \text{ cm}$, which can be comparable to the inner scale of the turbulence (Spangler & Gwinn 1990; Kaspi & Stinebring 1992; Gupta, Rickett & Coles 1993) where the statistics of the ISM are different from the statistics responsible for pulse broadening. The visibility function can be easily constructed in our multi-screen model by solving Eqs. (4,6) for $\Delta k = 0$, however, we leave its analysis for future communication. Here, we estimate what restrictions would be imposed on our theory by an inner scale of the order $y_{in} \sim 10^8 \text{ cm}$.

Due to the formulas of Section 3, large-angle refraction is provided by small-scale fluctuations of electron density. In the case of Lévy statistics, a sum of random variables can be dominated by a single term, therefore, from formula (17) we can estimate $(\Delta\tilde{\xi}_{max})^2 \sim 2\pi\tau c/(z_0 N \lambda^2 B^2)$. From formula (15), the electron-density fluctuations producing such an angle deviation should be strong at the scale $y_{min} \sim 2\pi/(B\Delta\tilde{\xi}_{max}) \sim [2\lambda^2 N z_0/(\tau c)]^{1/2}$, or

$$y_{min} \sim \sqrt{\frac{2cDM}{\langle n \rangle \tau \nu^2}}, \quad (22)$$

where we introduced the dispersion measure $DM = \langle n \rangle N z_0$, and the signal frequency, $\nu = c/\lambda$. Quite conveniently, formula (22) includes only the quantities averaged along the line of sight, but not the particular parameters l , l_0 , Δn_0 , and α of the scattering screens.

As an example, let us consider the parameters for the large-dispersion-measure pulsar J1852+0031 (DM=680.0) observed at 1175 MHz in (Bhat *et al* 2004). Substituting $\nu \sim 10^9 \text{ s}^{-1}$, $DM \sim 2 \cdot 10^{21} \text{ cm}^{-2}$, $\tau \sim 0.5 \text{ s}$, and assuming that $\langle n \rangle \sim 3 \cdot 10^{-2} \text{ cm}^{-3}$, we obtain $y_{min} \sim 10^8 \text{ cm}$. Therefore, the condition $y_{min} \sim y_{in}$ is marginally satisfied. Due to the scaling $\tau \propto \lambda^4 DM^4$, smaller-dispersion-measure pulsars satisfy this condition even better. For the cases when this condition is violated, a more appropriate description will be given by “truncated” Lévy distributions, see e.g., (Nakao 2000).

In conclusion we would like to mention the observational correlation functions that are expressed through the higher-than-second moments of the wave amplitude, $\Phi(\mathbf{x}, t)$. These observational quantities require a special consideration that at present is not available to

us. The examples of such quantities are given by the frequency correlation function that is used to characterize pulse broadening for $DM < 100 \text{ pc cm}^{-3}$, see, e.g., (Gwinn *et al* 1998), or by the intensity correlation functions that are used to characterize the density statistics on scales larger than the Earth size (Shishov *et al* 2003). The scaling of such functions may be easily found in the Gaussian theory when these functions can be related to the second-order moment, $\langle (\Delta n)^2 \rangle$. However, the meaning of these correlation functions in the Lévy case has yet to be determined. For instance, it seems possible that the deviation of the pulse-width scaling from $\tau \propto DM^4$ for the lower part of the elbow diagram, in Fig. (1), is due to the different method of reconstructing τ in this region. Indeed, below $DM \sim 100 \text{ pc cm}^{-3}$, τ is not measured directly, but rather is defined as the inverse frequency decorrelation bandwidth (Sutton 1971; Rickett 1977, 1990; Ramachandran, *et al* 1997; Gwinn *et al* 1998; Bhat *et al* 2004).

To summarize, in the present paper we proposed a multi-screen model of the uniform, non-Gaussian interstellar medium, and we found its analytic solution. We demonstrate that this model explains both the shapes and the scalings of the observational pulse profiles, and it is free of the Sutton and Williamson paradoxes that could hardly be resolved in the standard Gaussian theory of scintillations. Also, we provided a physical model of density distribution having random discontinuities, which produces Lévy scintillations and which may serve as a good approximation for the analysis of the observational data. We have demonstrated that the observational pulse shapes depend on the entire shape of the distribution of electron density, rather than simply on the second moment. Pulse profiles may therefore serve as a valuable tool for reconstructing this function from observations, and we have developed the corresponding method in the present paper.

7. Acknowledgement

We are very grateful to Ramachandran Rajagopalan for allowing us to use the observational results published in (Ramachandran, *et al* 1997). We would like to thank John Nolan for his valuable advice on the method of numerical generation of symmetric stable distributions, and Fausto Cattaneo, Arieh Königl, and Robert Rosner for important discussions. S.B. would like to thank the Aspen Center for Physics where a part of this work was done. The work of S.B. was supported by the NSF Center for magnetic self-organization in astrophysical and laboratory plasmas, at the University of Chicago.

REFERENCES

Armstrong, J. W., Rickett, B. J., & Spangler, S. R. (1995) *ApJ* **443**, 209.

Bhat, N. D. R., Cordes, J. M., Camilo, F., Nice, D. J., & Lorimer, D. R. (2004) *ApJ* **605**, 759.

Bhat, N. D. R., Cordes, J. M., & Chatterjee, S. (2003) *ApJ* **584**, 782.

Blandford, R. & Narayan, R. (1985) *MNRAS* **213** 591.

Boldyrev, S. & Gwinn, C. R. (2003a) *ApJ* **584**, 791.

Boldyrev, S. & Gwinn, C. R. (2003b) *Phys. Rev. Lett.* **91** 131101.

Boldyrev, S. & Gwinn, C. R. (2004) *Astrophysics and Space Science* **292**, 147-153.

Boldyrev, S. (2002) *ApJ* **569**(2), 841.

Boldyrev, S., Nordlund, Å., & Padoan, P. (2002) *ApJ* **584** 791.

Chambers, J., Mallows, C., & Stuck, B., (1976) *Journal of American Statistical Association, Theory and Methods* **71**(354), 340-344.

Chandran, B. D. G. & Backer, D. C., (2002) *ApJ* **576**, 176.

Cho, J., Lazarian, A., & Vishniac, E. (2000) *ApJ* **564**, 291.

Constantin, P., Procaccia, I., & Sreenivasan, K. R. (1991) *Phys. Rev. Lett.* **67**, 1739.

Cordes, J. M., & Lazio, T. Joseph W. (2001) *ApJ* **549**, 997.

Desai, K.M., & Fey, A.L. (2001), *ApJS*, **133**, 395.

Elmegreen, B. & Falgarone, E. (1996) *ApJ* **471**, 816.

Feller, W. (1971) *An Introduction to Probability Theory and Its Applications* (John Wiley & Sons, Inc., New York), Ch. VI(2).

Fiedler, R.L., Dennison, B.J., Johnston, K.J., & Hewish, A. (1987), *Nature*, **326**, 675.

Goldreich, P. & Sridhar, S. (1997), *ApJ* **485**, 680.

Goodman, J. & Narayan, R. (1985) *MNRAS* **214** 519.

Gupta, Y., Rickett, B. J., & Coles, W. A. (1993) *ApJ* **403**, 183.

Gwinn, C. R. *et al* (1998), ApJ **505**, 928.

Hirano, C., Gwinn, C. R., & Boldyrev, S., (2002), astro-ph/0204367.

Jayannavar, A. M. & Kumar, N. (1982) Phys. Rev. Lett. **48**, 553.

Kaspi, V. M. & Stinebring, D. R. (1992) ApJ **392**, 530.

Klafter, J., Zumofen, G., & Shlesinger, M. S. (1995), in *Lévy flights and related topics in Physics* (Springer, Berlin).

Kraichnan, R. H. (1991), Phys. Rev. Lett. **67**, 3634.

Kritsuk, A. G. & Norman, M. L. (2004) ApJ **601**, L55-L58.

Lambert, H. C. & Rickett, B. J. (2000) ApJ **531**, 883.

Lee, L. C. & Jokipii, J. R. (1975a) ApJ **196**, 695.

Lee, L. C. & Jokipii, J. R. (1975b) ApJ **201**, 532.

Lee, L. C. & Jokipii, J. R. (1975c) ApJ **202**, 439.

Lithwick, Y. & Goldreich, P. (2001) ApJ **562**, 279.

Meneveau C. & Sreenivasan, K. R. (1990) Phys. Rev. A **41**, 2246.

Nakao, H., (2000), cond-mat/0002027.

Nolan, J. P., (2002) “Stable Distributions. Models for Heavy Tailed Data” (<http://academic2.american.edu/~jpnolan/stable/stable.html>).

Phillips, J. A. & Clegg, A. W., (1992), Nature **360**, 137.

Ramachandran, R., Mitra, D., Deshpande, A. A., McConnell, D. M., & Ables, J. G., (1997) MNRAS **290**, 260.

Rickett, B. J. (1977) Ann. Rev. Astron. Astrophys. **15**, 479.

Rickett, B. J. (1990) Ann. Rev. Astron. Astrophys. **28**, 561.

Rickett, B. J., Lyne, A. G., & Gupta, Y. (1997) MNRAS **297**, 739.

Romani, R. W., Blandford, R. D., & Cordes, J. M. (1987) Nature **328**, 324.

Saul, L., Kardar, M., & Read, N. (1992) Phys. Rev. A **45**, 8859.

Scalo, J. & Elmegreen, B. (2004) astro-ph/0404452; Ann. Rev. Astron. Astrophys., to appear.

Shishov V. I., *et al* (2003) A&A, **404** 557S.

Spangler, S. R. & Gwinn, C. R. (1990) ApJ **353**, L29-L32.

Stinebring, D.R., McLaughlin, M.A., Cordes, J.M., Becker, K.M., Goodman, J.E.E., Kramer, M.A., Scheckard, J.L, & Smith, C.T. (2001), ApJ **549**, L97.

Sutton, J. M. (1971) MNRAS, **155**, 51.

Tatarskii, V. I. (1961) *Wave Propagation in a Turbulent Medium* (New York, McGraw-Hill).

Uscinski, B. J. (1974), Proc. R. Soc. London, A **336**, 379.

Williamson, I. P. (1972) MNRAS, **157**, 55.

Williamson, I. P. (1973) MNRAS, **163**, 345.

Williamson, I. P. (1974) MNRAS, **166**, 499.

Williamson, I. P. (1975) Proc. R. Soc. London, A **342**, 131.

Wolszczan, A., & Cordes, J.M. (1987), ApJ, **320**, L35.

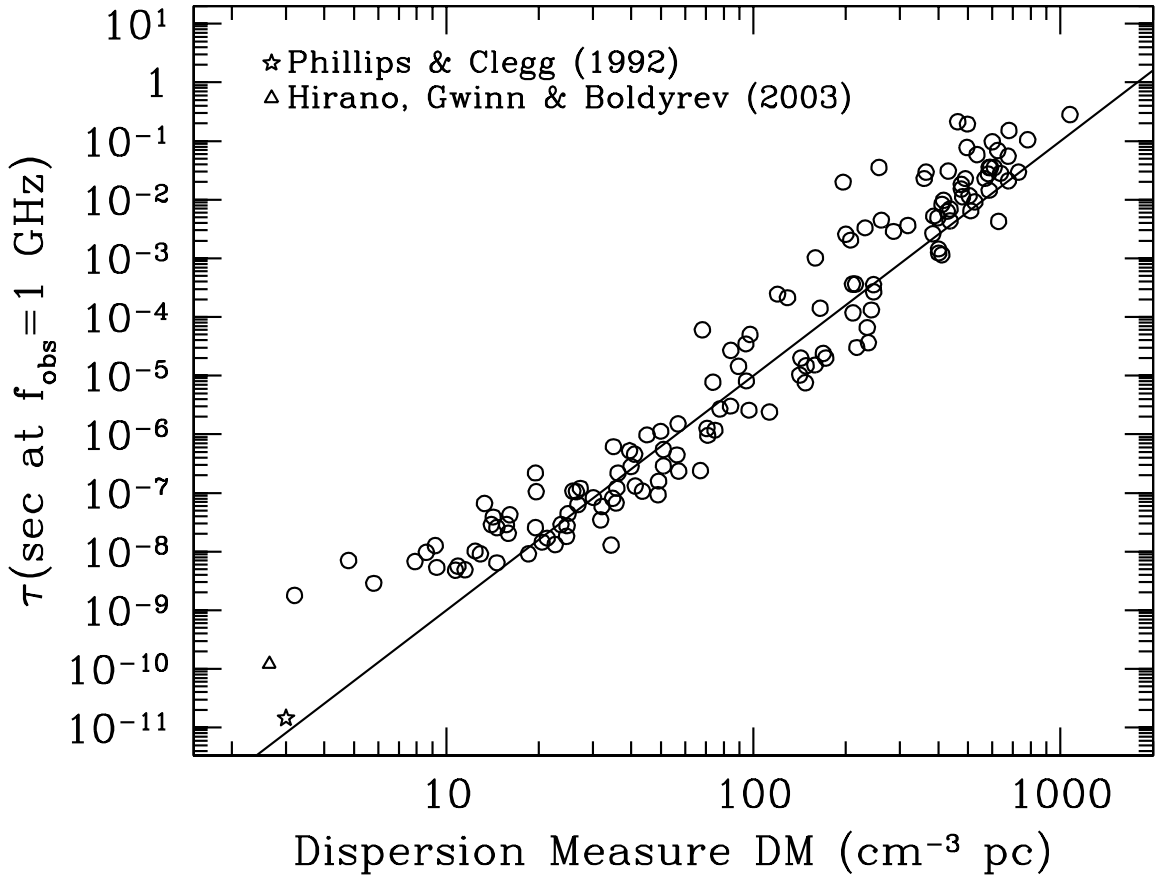


Fig. 1.— Pulse temporal broadening as a function of the dispersion measure, $DM = \int_0^d n(z) dz$, which is a measure of the distance to the pulsar. Except as noted, data were taken from (Phillips & Clegg 1992). The solid line has slope 4, which contradicts the standard Gaussian model of scintillations predicting slope 2 (the Sutton paradox), and which agrees with the Lévy model with $\beta = 2/3$.

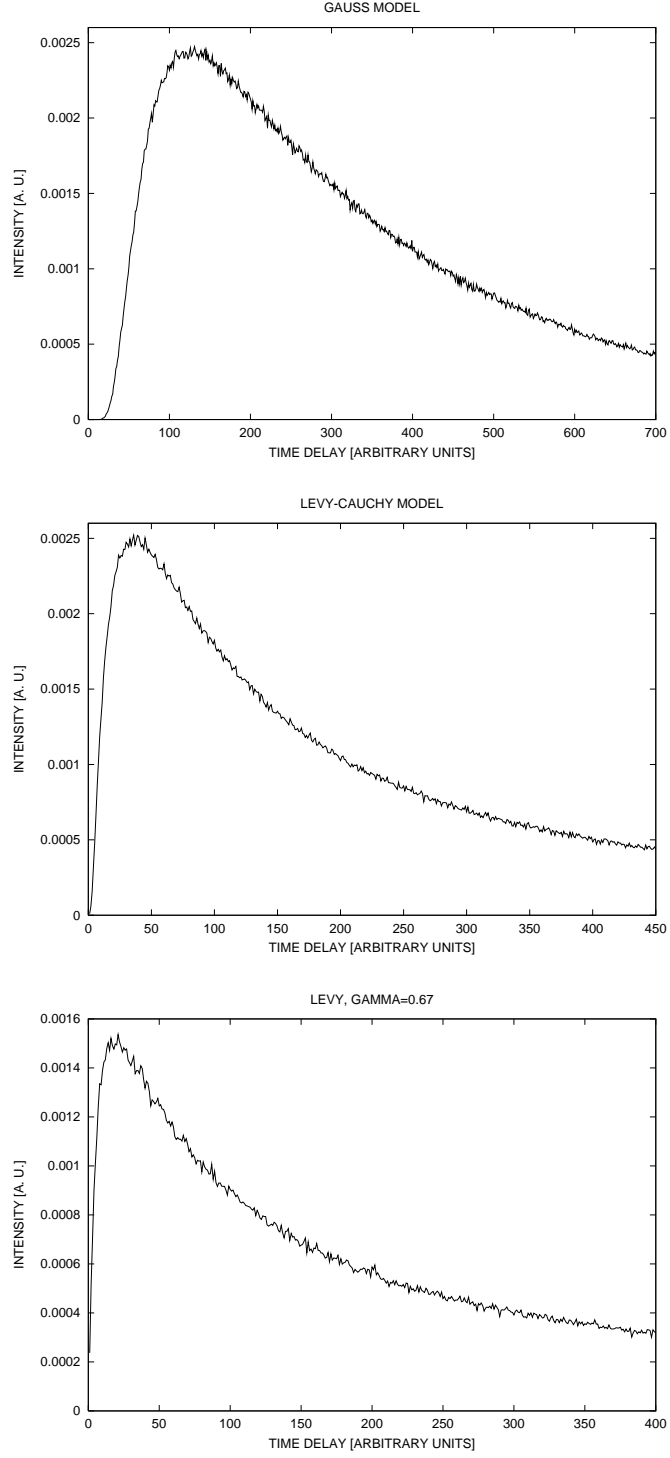


Fig. 2.— Intensities of pulses predicted by the Gaussian model ($\gamma = 2$), by the Lévy-Cauchy model ($\gamma = 1$), and by the Lévy model with $\gamma = 2/3$, for statistically uniform distribution of electron density in the interstellar medium. Note the sharp rise and the pointed apex of the signal predicted by the Lévy model compared to the signal predicted by the Gaussian model. The shapes are rescaled to have similar decaying parts.

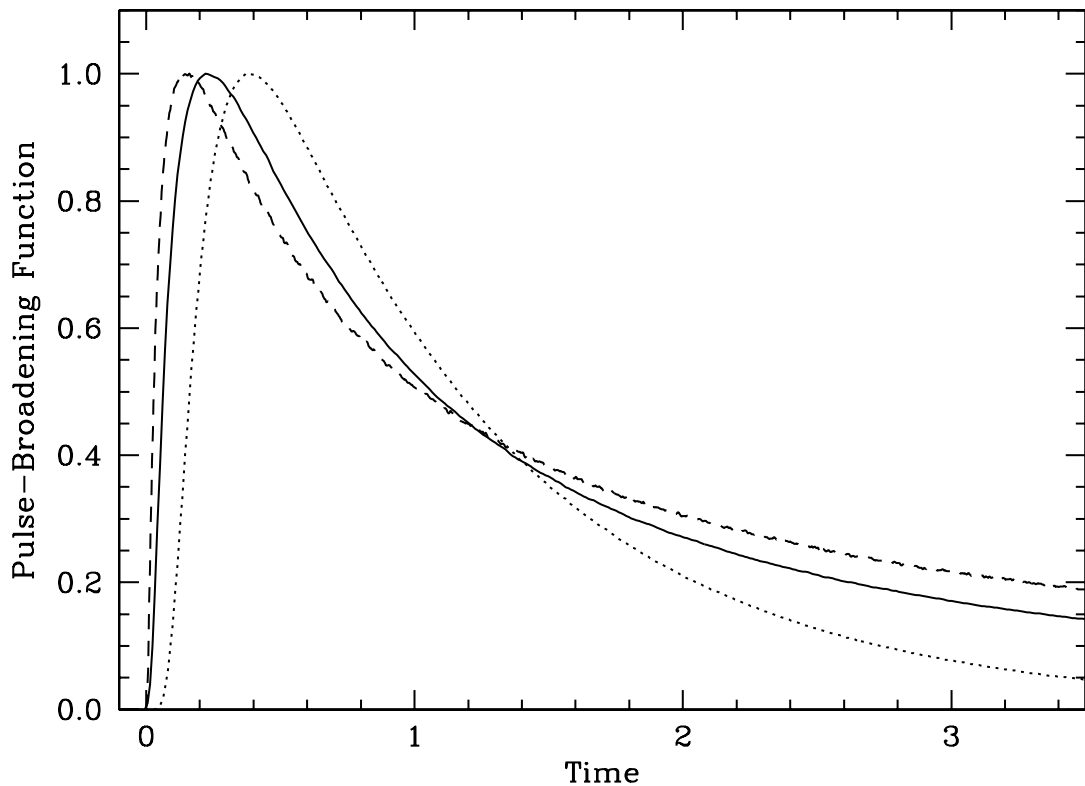


Fig. 3.— Pulse broadening function for $\gamma = 2/3$ (dashed line), $\gamma = 1$ (Cauchy: solid line), and $\gamma = 2$ (Gaussian: dotted line). The unscattered signal would arrive at time $t = 0$. Note the different relative arrival times of the peaks, as well as the different power-law behavior in the tail, for different values of γ . The shapes are rescaled to have same amplitudes and half-widths.

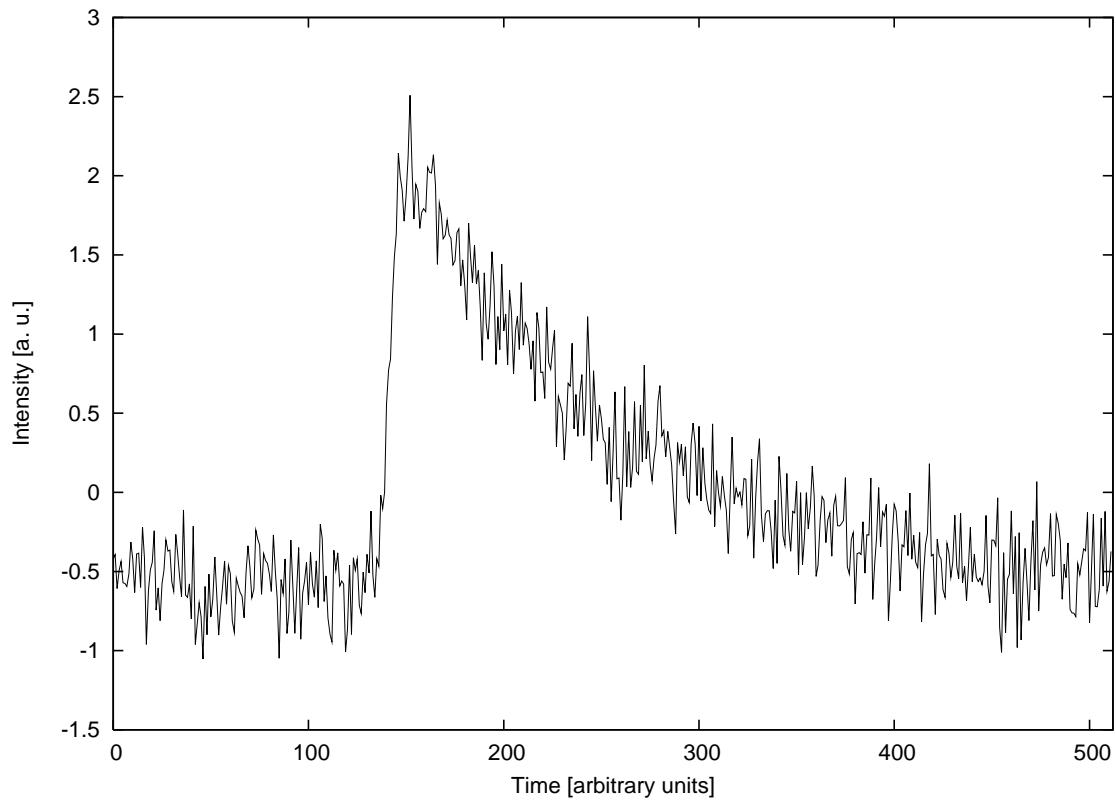


Fig. 4.— The pulse shape of the pulsar J1848-0123, obtained by Ramachandran, Mitra, Deshpande, Connell, & Ables (1997) (Courtesy of Ramachandran Rajagopalan). The data are obtained with the Ooty Radio telescope at 327 MHz. Note the sharp rise and the pointed apex of the signal.

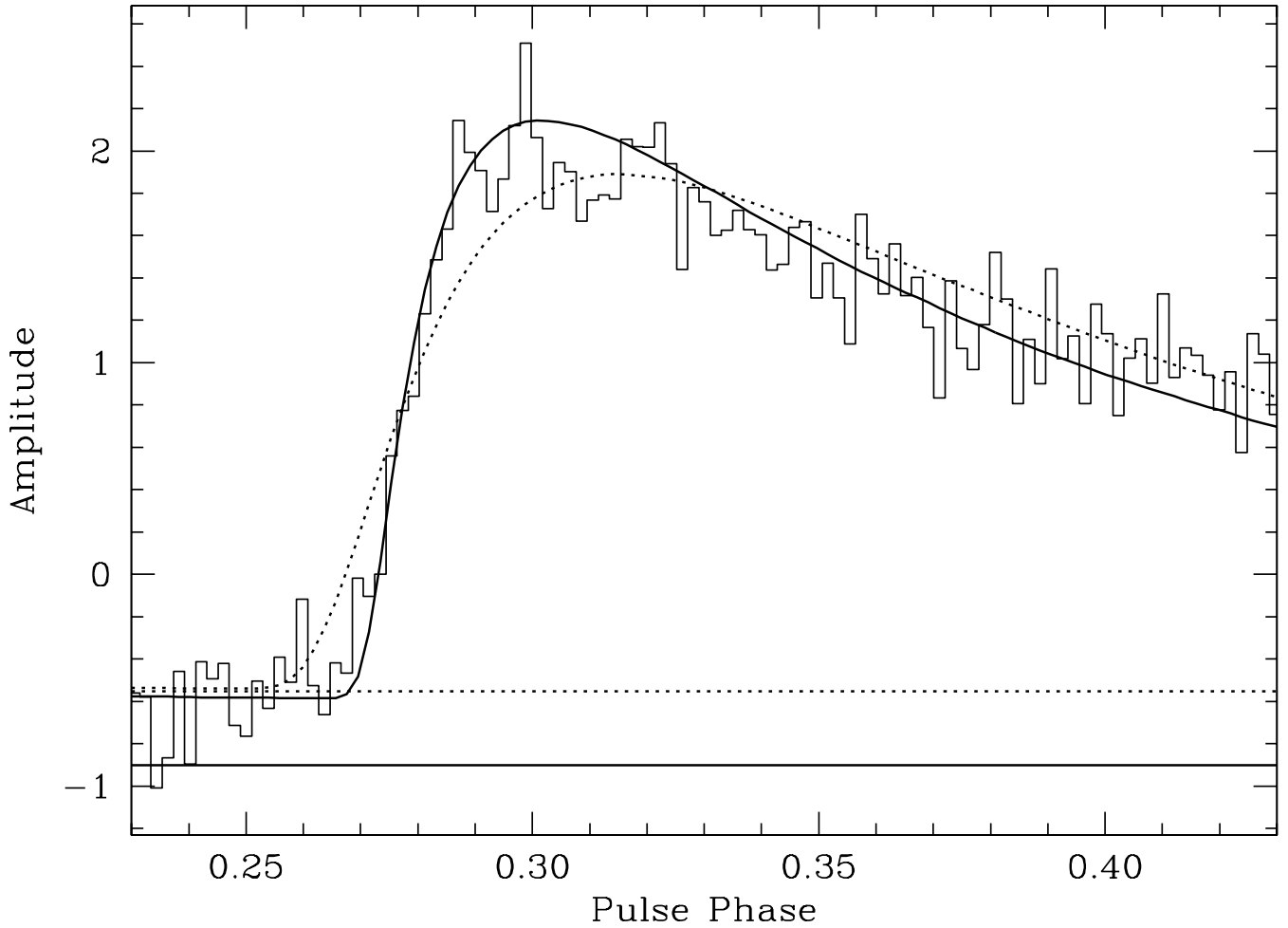


Fig. 5.— Best-fitting pulse-broadening functions for the pulse of pulsar J1848-0123. Solid line: $\gamma = 1$ (Cauchy), dotted line: $\gamma = 2$ (Gaussian). Histogram shows the pulse obtained by Ramachandran et al. (1997). [Courtesy of Ramachandran Rajagopalan.] Horizontal lines at bottom show the zero levels for the two functions; note that the intensity never reaches zero for $\gamma = 1$, as a consequence of overscattering. Also note that the Cauchy curve yields a steeper rise and a sharper peak, in agreement with the data.